Journal of Applied Sciences and Nanotechnology, Vol. 3, No. 1 (2023)

Journal of Applied Sciences and Nanotechnology

Journal homepage: https://jasn.uotechnology.edu.iq/

Preparing and Investigating the Structural Properties of Porous Ceramic Nano-Ferrite Composites

[1]Huda Jabbar*, [1]Enas Muhi, [2]Tahseen Hussien

[1]Branch of Materials Science, Department of Applied Sciences, University of Technology – Iraq

[2]Department of Physics, University of Diyala – Iraq

Article information

Article history:
Received: March, 12, 2022
Accepted: August, 25, 2022
Available Online: March, 10, 2023

Keywords:
Nano ferrite,
Porous Ceramic,
Porosity,
Diametrical Strength

Corresponding Author:
Huda Jabbar
Huda.J.abdulhussein@uotechonolgy.edu.iq

Abstract:
Highly porous kaolin ceramics composites were produced by adding space-holder materials during dry pressing. To increase the strength of porous kaolin ceramic composites different ratios of cobalt-nickel ferrite nanoparticles (5, 10, 15, and 20%) were added. The sol-gel auto-combustion method prepared the nano cobalt-nickel ferrite particles (CNF). Space-holder materials were removed by preheating, and solid specimens were produced by sintering. X-ray diffraction (X-RD) and Fourier transform infrared spectroscopy (FT-IR) was used to examine the structural characteristics. Up to 47.05% porosity was achieved when 20% CNF was added to the porous kaolin ceramics composites. The results indicated that the higher percentages of nano CNF 20% decreased linear shrinkage and the loss of ignition by 4.4% and 30.4%, respectively. While increased apparent density and diametrical strength of 1.42 g/cm^3, and 9.03MPa respectively. Diametrical strength nanoparticles increased the strength attributed to the formation of a secondary phase in the porous ceramics, improving the crack bridging mechanism.

DOI: 10.53293/jasn.2022.4804.1150, Department of Applied Sciences, University of Technology

1. Introduction

Porous ceramics have received a lot of attention, and are commonly used in a variety of fields, including hot corrosive gas filtration, water filtration, molten metal filtration catalyst carriers, solid oxide fuel cells, and thermal insulators [1-7]. During the manufacturing of materials, porous materials can be created inadvertently or deliberately [8]. The characteristics of porous ceramic materials, such as lightweight, low density, thermal stability, and high resistance to chemical attack have applications in a variety of fields [9]. For porous ceramics to perform the desired role in a specific application environment, the distribution of void space sizes, shapes, and volumes should be controlled [10, 11]. Recent technical advancements, as well as the need for new functions, have created a large market for novel materials. Compared to their pure equivalents, mixtures between materials may have better properties [12]. For example, spintronic materials exhibit both magnetic and semiconducting properties. The incorporation of a basic structural material into a second substance may produce these mixtures or hybrid structures. Porous materials seem to be appropriate candidates for this application [13, 14]. Ferrites are well-known ferrimagnetic materials, which possess unique electromagnetic properties, high electrical resistivity, controllable saturation magnetization, moderate thermal expansion coefficients, and energy-transfer efficiency

[15-18]. There is a variety of physical or chemical methods employed to prepare the spinel-type ferrite such as the sol-gel auto-combustion method [19], chemical precipitation [20], or mechanical mixing procedure [21]. In this paper, porous dispersion ceramic composites were synthesized from kaolin, palm fronds as pore-forming agents, and cobalt-nickel ferrite nanoparticles. The focal objective of this work is to study the effect of Nano CNF addition on the physical and mechanical properties of porous kaolin ceramic composite.

2. Experimental Procedure

2.1. Materials

The raw materials (kaolin) for this research were obtained from the western desert (Dwekhla) in Iraq. Table 1 listed the chemical analysis of kaolin. Using a ball mill, the kaolin was ground and sieved to a particle diameter of 75µm. The palm fronds powder (with particle size 0.3µm) was used as space-holder materials. Cobalt-nickel ferrite nanoparticles (with an average particle size of 53–46 nm) were used as nanoadditives.

Table 1: Chemical analysis of kaolin.

Oxide	SiO_2	Al_2O_3	Fe_2O_3	CaO	TiO_2	K_2O	Na_2O	Mgo	L.O.I
kaolin wt.%	49.38	32.72	2.07	1.19	1.08	0.44	0.22	0.18	12.42

2.2. Fabrication of Magnetic Dispersion Porous Ceramic

The preparation of dispersion porous ceramic composite involves several steps. The first involves selecting the optimum value of palm fronds added to kaolin. Then the optimum value of CNF selects. The third step includes the addition of CNF with different weights (0, 5, 10, 15, 20) wt.% to the mixture (kaolin-palm fronds), and the mixtures were also dry pressed into disk shapes (20mm diameter and 2mm thickness) shown in Figure 1. Following that, a programmable furnace "Nabertherm-p310-Germany" is used to sinter the material at (1100 ^{o}C) for two hours. Table 2 shows the weight ratios of prepared specimens.

Figure 1: Photograph of prepared specimens after sintering

Table 2: Weight ratios of prepared magnetic dispersion porous ceramic specimens.

Code of specimen	Kaolin +P.F content wt%	CNF content wt%
F1	100	0
F2	95	5
F3	90	10
F4	85	15
F5	80	20

X-ray Diffraction analysis was used to determine the phases present in the specimens. FTIR spectroscopy in the range of 400 to 4000 cm^{-1} was measured at room temperature. ASTM (C1407, 326) uses to calculate the loss of ignition and linear shrinkage, respectively. The loss of ignition and linear shrinkage is calculated by the following Eqs. (1) and (2), respectively [21].

$$\boldsymbol{L.M} = \frac{\boldsymbol{Mo-M}}{\boldsymbol{Mo}} \quad (1)$$

Where, Mo is the initial mass of the specimen before firing (g), and M is the final mass of the specimen after firing (g) [22].

$$(\boldsymbol{l.sh}\%) = \frac{\boldsymbol{lo-l}}{\boldsymbol{lo}} \times \mathbf{100}\% \quad (2)$$

l_o is specimen length before firing, l is specimen length when fired. ASTM(C373) uses the Archimedes drainage method to calculate (A.P.) apparent porosity, (W.A.) water absorption, and (A.D) apparent density. The apparent porosity and apparent density are estimated using Eqs. (3), and (4), respectively [23].

$$(\boldsymbol{A.P.})\% = \frac{\boldsymbol{Ws-Wd}}{\boldsymbol{Ws-Wi}} \times \mathbf{100}\% \quad (3)$$

$$(\boldsymbol{A.D}\ \%) = \frac{\boldsymbol{Wd}}{\boldsymbol{Ws-Wi}} \quad (4)$$

W_s is the soaked specimen (g), W_i is the suspended specimen (g), and W_d is the dry specimen (g). b is the diametrical strength (σ_D) of all specimens was determined using the Brazilian disk testing. (ASTM-C773) was used to calculate diametrical strength by the following Eq. (6) [22].

$$\boldsymbol{\sigma_D} = \frac{\boldsymbol{2F}}{\boldsymbol{\pi dD}} \quad (5)$$

F is load(N), d is the length of specimens(mm), and D is the diameter of specimens (mm)

3. Results and Discussion

3.1.XRD pattern of dispersion porous ceramic composite

Figure 2 displays the X-Ray diffraction of the synthesized specimens. The major phase of the specimen (F1) is mullite, and the cristobalite phase is the second phase since it contains a lot of kaolin, which means it has a lot of mullite. XRD of magnetic porous ceramic with CNF ratios of (5, 10, 15, and 20) wt.% showed a cubic spinel structure of CNF with seven peaks (311), (222), (400), (422), (511), (440) and (622) that do not reveal the presence of any other phase in the specimens, located at 2θ = 35.64°, 37.28°, 43.3°, 39.72°, 57.23°, 62.91°, and 74.56°, respectively. It can be seen that the most intense peak is (311) in all specimens. The intensity of the peak, especially the preferred plane, increased with increasing the CNF content, and the intensity of the mullite phase decreased with increasing the CNF, which resulted in decreasing the raw kaolin. The addition of CNF may lead to the atrophy of some phases in porous ceramics.

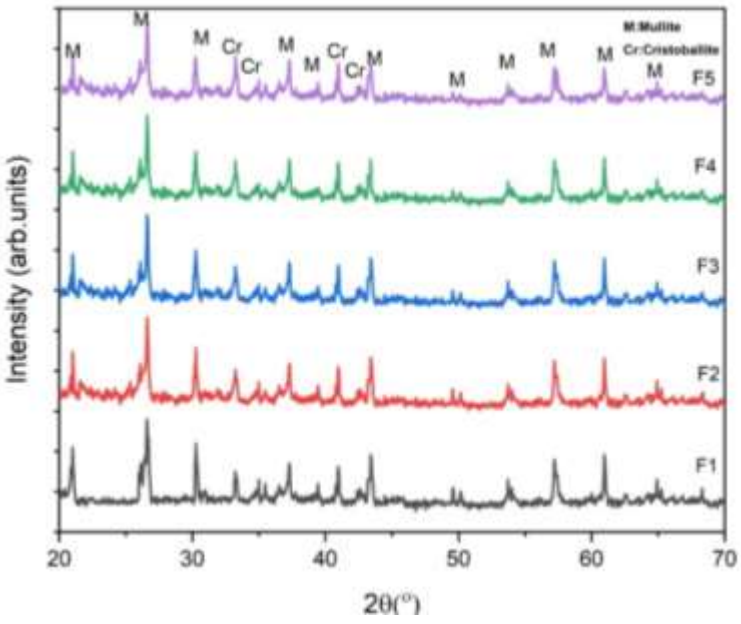

Figure 2: The XRD pattern of the prepared specimens.

3.2. FTIR of Dispersion Porous Ceramic Composite

Figure 3 represents the FT-IR spectrum of a dispersion porous ceramic composite. The magnetic properties of CNF powder prepared at pH = 9 and sintering temperature of 1100°Care optimal. The peaks observed in the range 486.0616-493.7768cm^{-1}, are related to octahedral complexes, while the peaks observed in the range 561.2854– 569.0007cm^{-1}, are related to tetrahedral complexes that showed the spinal structure of CNF in the porous ceramic. The bands that have been found within the range 798.25–909.87cm^{-1} are related to AL-O stretching and the peak at 1070.53cm^{-1} is anti-symmetric stretching vibrations of the Si–O–Si in amorphous silica and Si–O–Al networks. C-O stretching is responsible for the bands found at 1095.53cm^{-1} as a specimen, 1128.39cm^{-1} for 5% CNF, 10% CNF, 1130.32cm^{-1} for 15% CNF, and 1126.47cm^{-1} for 20% CNF. The CO_2 absorption is observed at around 1519.59–1557.27cm^{-1}. The band about 3664.75cm^{-1} as the specimen where the peak is located at a range 3748.28 -3754.45cm^{-1} is attributed to Si–O–H vibration. The band observed at 2360.23-2365.65cm^{-1} is related to the aliphatic and aromatic C–H stretching bonds. Other peaks found in the range 2852.23–2945.06cm^{-1} are attributed to C-H stretching bands. The weak peaks observed in the range 3444.98–3680.41cm^{-1} are related to the hydroxyl group's stretching vibration. Table 3 displays the FTIR spectrum for the magnetic porous ceramic specimens with different weight ratios of CNF.

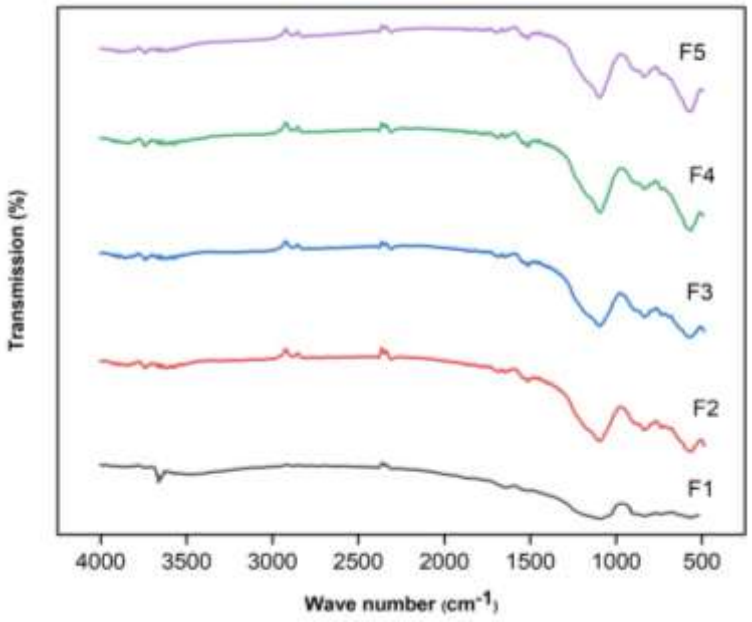

Figure 3: FTIR of the prepared specimens.

Table 3: FT-IR spectral bands of prepared specimens.

Sample	Weight ratio	FTIR frequency bands (cm^{-1})	
		ν_1	ν_2
F1	0	----------	----------
F2	5	561.2854	486.0616
F3	10	565.1430	487.9904
F4	15	567.0719	491.84808
F5	20	569.0007	493.7768

3.3. Physical Properties

3.3.1. Loss of Ignition

The influence of nano additions on the porosity and mass loss of a dispersion porous ceramic composite at a constant amount of palm fronds is plotted in Figure 4, which demonstrates the apparent porosity and loss of ignition against the weight fraction of CNF nanoparticles. The apparent porosity is 58.34%, 46.78%, and

47.05%, respectively, and the loss of ignition is 40.03%, 32.5%, and 30.4%, respectively. Reducing the kaolin content caused a reduction in loss of ignition, which is caused by burning loss of lattice water and impurities, so decreasing the kaolin ratio causes a decrease in loss of ignition and porosity, and these behaviours degree [22]. On the other hand, adding nanoparticles to porous ceramic reduces porosity and the loss of ignition [24].

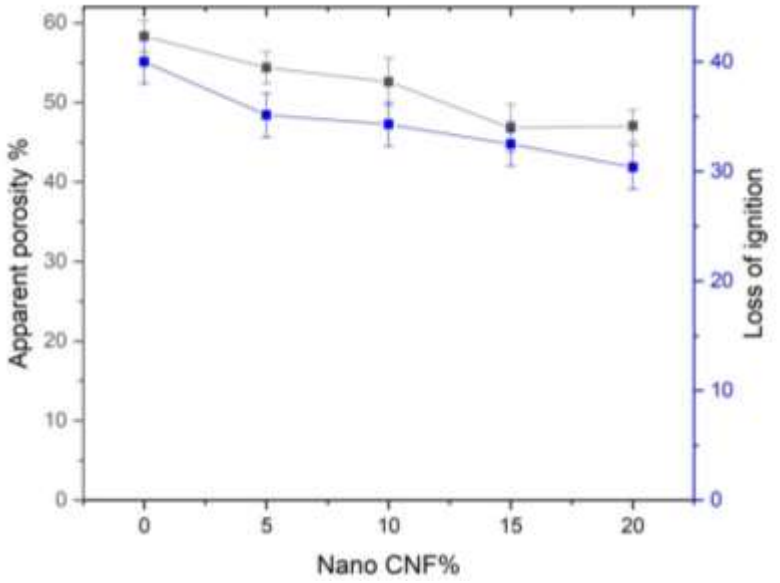

Figure 4: Effect of (CNF) ratios on the porosity and loss of ignition for specimens.

3.3.2. Linear Shrinkage and Apparent Density

Figure 5 depicts the linear shrinkage and apparent density of nano CNF specimens after sintering at 1100 ^{o}C. From Figure 5, it's obvious that adding CNF nanoparticles increases density, which is measured to be about 0.99, 1.35, and 1.42 g/cm^3 respectively. The increase in apparent density could be a result of CNF agglomeration and closed pores [25]. During drying, linear shrinkage happens after water is evaporated from the surface and voids inside specimens. When the water is replaced by air, the particulates touch each other. Linear shrinkage depends on the mineralogical composition, shaping, and drying process [20]. In our case, results showed that the minimum and maximum linear shrinkages were 4.4 and 6.04% respectively. Reduction in kaolin is an agent that reduces linear shrinkage by reducing the amount of liquid phase that causes shrinkage of this degree [24,26].

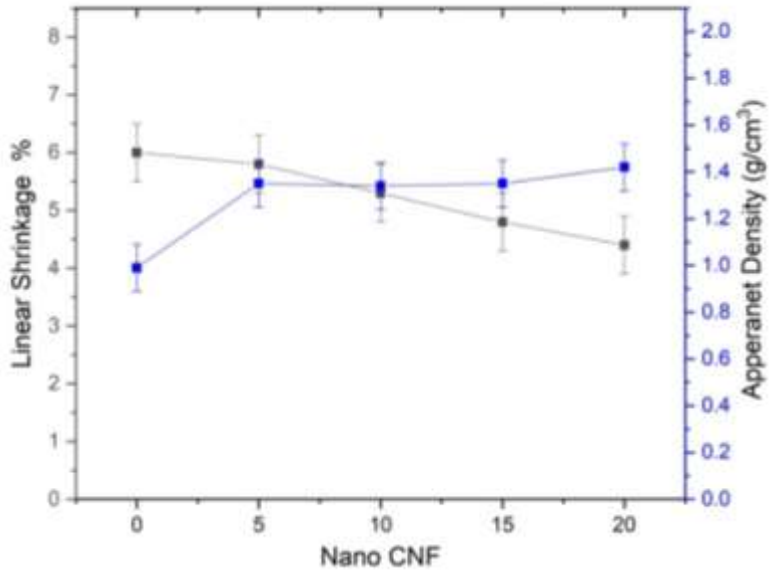

Figure 5: Effects of CNF ratios on the Linear Shrinkage and apparent density of specimens.

3.4. Mechanical Properties

3.4.1. Diametrical Strength

Figure 6 displays the effect of added nano CNF on the porosity and diametrical strength of the dispersion porous ceramic composite. It was noticed that diametrical strength increased from 2.33MPa to 9.03MPa as the wt.% by addition of 20 wt.% of CNF nanoparticles. This behaviour is affected by the presence of CNF in the kaolin matrix, which prevents dislocation motion and grain boundary migration, resulting in reduced grain growth [27]. The value of porosity decreased from 58.34% to 47.04% because the pores were filled by CNF. The formation of more bonds in the initial green compact due to the greater content of CNF particles and the production of ceramic phases including CNF-$AL_2O_3.2SiO_2$, improves the crack bridging mechanism [28]. Table 4 displays a comparison between the current study and previous studies.

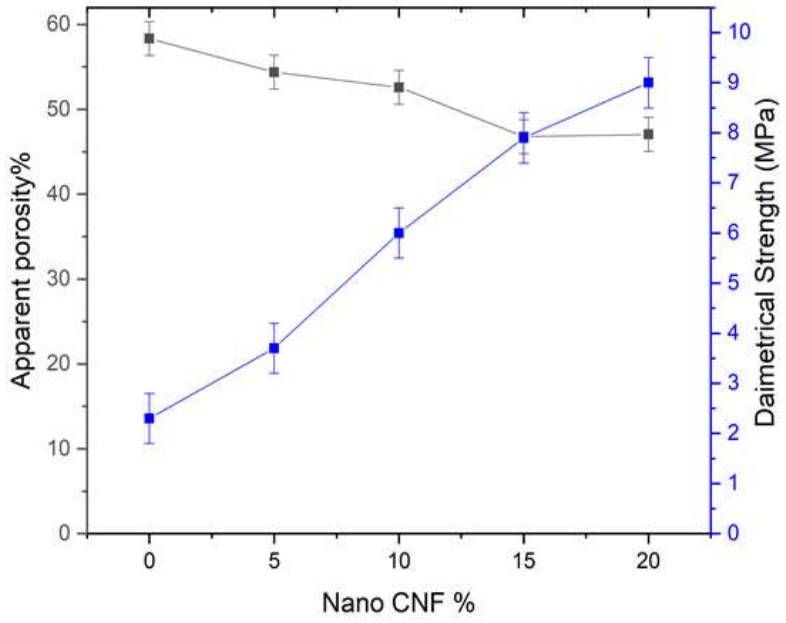

Figure 6: Effect of (CNF) ratios on the Porosity and diametrical Strength of specimens.

Table 4: Comparison between the current study and previous studies.

Researchers	Raw materials	Porosity	Mechanical strength	Cost
Al-Attar et al. [24]	Porous alumina-zirconia and nano-additives	42-30%	Increased with increasing nanoadditives	high
Sabah et al. [21]	Alumina and nano-copper	30.7-24.54%	Increased with increasing nano-copper	high
current study	porous kaolin and CNF	58.34-47.05%	Increased with increasing CNF	low

4. Conclusions

The porous kaolin ceramic composites dispersed with CNF were successfully manufactured. The effect of the nano-additive of CNF on the porosity, loss of ignition, density, and diametrical strength was examined. XRD analysis revealed variations in the phase of precursor materials. The porosity and linear shrinkage decrease with the increase in the ratios of CNF from 58.34-47.05% to 6.04-4.4%, respectively. While apparent density and diametrical strength are increasing. The results back up the idea that CNF is used as a secondary phase in porous ceramics to improve mechanical properties and control the porosity at the nanoscale. The porous ceramic nano ferrite composites synthesized in this study is compared with that of other materials in Table 4. The results showed excellent mechanical properties and high porosity. This study identifies a cost-effective approach to porous ceramic nano ferrite composites from kaolin with palm frond as pore former.

Conflict of Interest

There are no financial or other conflicts of interest declared by the authors.

References

[1] V.G. Resmi, V. Lakshmi, M. Brahmakumar, and T.P. Rajan, "Processing of silica bonded porous SiC perform for metallic composites," *J. Porous Mater*. vol.22,pp.1445–1454, 2015.

[2] W. Hussain, E. Muhi, and M. Ismail, "Preparation of Household Water Filter," *Journal of Applied Science and Engineering*, vol. 23, pp. 61-68 ,2020.

[3] N. M. Al Muhamad, L. C. Hong, Z. A. Ahmad, and H. M.Akil, "Preparation and characterization of ceramic foam produced via polymeric foam replication method," *Journal of materials processing technology* ,vol.207, pp.235-239,2008.

[4] M. Fukushima and Y. Yoshizawa, "Fabrication of highly porous silica thermal insulators prepared by gelation- freezing route, "*J. Am. Ceram. Soc*. vol.97,pp.713-717,2014.

[5] W. Yan, N. Li, and B. Han, "Effects of sintering temperature on pore characterisation and strength of porous corundum-mullite ceramics," *Journal of Ceramic Processing Research*, vol. 11, pp. 388–391, 2010.

[6] J. Cao, J. Lu, L. Jiang, and Z.Wang, "Sinterability, microstructure and compressive strength of porous glass-ceramics from metallurgical silicon slag and waste glass," *Ceramics International*, vol. 42, pp. 10079–10084, 2016.

[7] F. Hasan and E. Muhi, " Study of the Mechanical and Thermal Properties of Refractory Mortars from Kaolin and Bentonite", *Journal of Applied Sciences and Nanotechnology*, vol. 2, pp.69-79, 2022.

[8] K. Hua, A. Shui, L. Xu, K. Zhao, Q. Zhou, and X. Xi, "Fabrication and characterization of anorthite–mullite–corundum porous ceramics from construction waste," *Ceramics International*, vol. 42, pp. 6080–6087, 2016.

[9] L. Shalal and S. Zaidan, "Structural Properties of Porous Silicon Carbide Bonded with Bentonite, Prepared by a Gas-Emitting Chemical Reaction Method," *Materials Science and Engineering*, vol.1049,pp.1-7,2021.

[10] K. Mohanta, A. Kumar, O. Parkash, and D. Kumar, "Processing and properties of low cost macroporous alumina ceramics with tailored porosity and pore size fabricated using rice husk and sucrose," *Journal of the European Ceramic Society*, vol. 34, pp. 2401–2412, 2014.

[11] F.Chen and L.Zhang, "Pore structure control of starch processed silicon nitride porous ceramics with near-zero shrinkage," *Materials Letters*, vol.65, pp.1410–1412,2011.

[12] A. Aramide and F. Tishin, "Production and Characterisation of Porous Insulating Fired Bricks from Ifon Clay with Varied Sawdust Admixture," *Journal of Minerals and Materials Characterisation and Engineering*, vol.11, pp.970-975,2012.

[13] C. Grish, R.Srivastavab, and V.Reddyc, "Effect of sintering temperature on magnetization and Mössbauer parameters of cobalt ferrite nanoparticles," *J of Mag. and Mag. Mater*. vol.427, pp.225–229, 2017.

[14] P. Raju and S.Murthy, "Preparation and characterization of Ni–Zn ferrite + polymer nanocomposites using mechanical milling method," *Appl. Nanosci*. vol.3, pp.469–475,2013.

[15] Z. Ali and R. Rasheed, "Preparation of V_2O_5 and SnO_2 Nanoparticles and Their Application as Pollutant Removal," *Journal of Applied Sciences and Nanotechnology*, vol. 1, pp.69-80, 2021.

[16] S. Salim, R. Al-Anbari, and A. Haider, "Polysulfone/TiO_2 Thin Film Nanocomposite for Commercial Ultrafiltration Membranes," *Journal of Applied Sciences and Nanotechnology*, vol. 2, pp.80-89, 2022.

[17] S. N. Kane, S. Raghuvanshi , and M. Satalkar, " Synthesis, Characterization And Antistructure Modeling Of Ni Nano Ferrite," *American Institute of Physics*,vol.23,pp.173-180,2018.

[18] M. Amir, A. Baykal, S. Güner, M. Sertkol, and M. Torak, "Synthesis and Characterization $Co_xZn - AlFeO_4$Nano particles," *Journal of Inorganic and Organometallic Polymers and Materials*, vol. 25, pp. 747-754, 2015.

[19] L. Sun and J. Wang, "Synthesis and characterization of porous Y_2SiO_5 with low linear shrinkage, high porosity and high strength," *Ceramics International*. vol .42,pp. 14894–14902,2016.

[20] R. Jabbar, S. H. Sabeeh, and A. M. Hameed. "Structural, dielectric and magnetic properties of Mn+2 doped cobalt ferrite nanoparticles", *Journal of Magnetism and Magnetic Materials*, vol. 494,pp.1-7, 2020.

[21] M. Sabah, M. A. Azmah, and S. M. Tahir, "The Effect of Commercial Rice Husk AshAdditives on the Porosity, Mechanical Properties,and Microstructure of Alumina Ceramics," *Advances in Materials Science and Engineering*, vol.20,pp22-32, 2017.

[22] E. Muhi and S.Luay, "Production of Water Filter from Porcelanite by Dry pressing," *Diyala Journal for Pure Science*,vol.17,pp.1-18,2021.

[23] H. Jabbar, E. Muhi, and T. Hussien, "Production Ceramic Crude Petroleum Filters from Local Raw Materials," *Materials Science Forum*, vol. 1039, pp. 96-103, 2021.

[24] M. Zawrah, S. Abo Sawan, and R. Khatta, "Effect of nano sand on the properties of metakaolin-based geopolymer:Study on its low rate sintering," *Construction and Building Materials*,vol.246,pp1-11, 2020.

[25] M. Hanoon, A. Al-Attar, and A. Resen, "Effects of SiC, SiO_2 and CNTs nanoadditives on the properties of porous alumina-zirconia ceramics produced by a hybrid freeze casting-space holder method," *Journal of the European Ceramic Society*, vol. 36, pp.1189-1195, 2016.

[26] E. Muhi and S. Issa, "A sustainable method for Porous refractory ceramic Manufacturing from kaolin by adding of burned and raw wheat straw," *Energy Procedia* ,vol.157, pp.241–253,2019.

[27] S. Irhayyim, H. Hammood, and H. Abdulhadi, "Effect of nano-TiO_2 particles on mechanical performance of Al–CNT matrix composite," *AIMS Materials Science*, vol.6,pp. 1124-1134,2019.

[28] M. Ali , M. A. Azmah, and S. M. Tahir, "The effect of nano-copper additives on the porosity, mechanical properties, and microstructure of alumina ceramics using commercial rice husk ash as a pore former", *Journal of the Australian Ceramic Society*, vol. 53, pp.963–974, 2017.